Copyright © 1988, by the author(s).
All rights reserved.

Permission to make digital or hard copies of all or part of this work for personal or classroom use is granted without fee provided that copies are not made or distributed for profit or commercial advantage and that copies bear this notice and the full citation on the first page. To copy otherwise, to republish, to post on servers or to redistribute to lists, requires prior specific permission.

DIFFUSION THROUGH A STOCHASTIC WEB

by

Allan J. Lichtenberg and Blake P. Wood

Memorandum No. UCB/ERL M88/48

6 July 1988

COVER PAGE

DIFFUSION THROUGH A STOCHASTIC WEB

by

Allan J. Lichtenberg and Blake P. Wood

Memorandum No. UCB/ERL M88/48

6 July 1988

ELECTRONICS RESEARCH LABORATORY

College of Engineering
University of California, Berkeley
94720

TITLE PAGE

DIFFUSION THROUGH A STOCHASTIC WEB

by

Allan J. Lichtenberg and Blake P. Wood

Memorandum No. UCB/ERL M88/48

6 July 1988

ELECTRONICS RESEARCH LABORATORY

College of Engineering
University of California, Berkeley
94720

Diffusion through a Stochastic Web

by

Allan J. Lichtenberg and Blake P. Wood

Department of Electrical Engineering and Computer Sciences
and the Electronics Research Laboratory
University of California, Berkeley, CA 94720

Abstract

A connected web of stochasticity can be generated by a mapping derived from a linear oscillator perturbed by a periodic delta-function. Such a stochastic web is useful for investigating global diffusion through a phase space in which the local diffusion within the web is nonuniform. An analytic expression for the global diffusion rate has been obtained using: (1) the basic phase space concept that the ergodic region is uniformly populated in the asymptotic limit, (2) a local calculation of the thickness of the stochastic web, and the (3) the average local period for traversing a single mesh of the web. The results are compared with numerical computations of the diffusion rate and found to be in good agreement. Although the linearity of the kicked oscillator leads to a connected grid in phase space, the diffusion rate, unlike Arnol'd diffusion, is related to that in two-dimensional phase space, with the diffusion coefficient $D_{web} \equiv L_{rms}{}^2/T$ scaling as K_α^3, where K_α is a perturbation parameter. Discrepancies are discussed, and the effect of extrinsic stochasticity is briefly considered.

1. Introduction

The motion of a charged particle gyrating in a magnetic field and interacting with a wave propagating perpendicular to the field is governed, within the non-relativistic approximation, by the equation

$$\ddot{x}+\omega_c x = \frac{e}{m}E_0 \sin(kx-\omega t). \tag{1}$$

Here x (and y) are transverse to the magnetic field $\hat{z}B_0$, the wave has amplitude $\hat{y}E_0$ and propagates in x with frequency ω and wave number k, and $\omega_c = eB_0/m$ is the gyrofrequency of the particle. The dynamics of this motion has been studied in some detail[1,2,3] and it has been shown that for exact resonance between the gyromotion and the applied frequency

$$\frac{\omega_c}{\omega} = \frac{p}{q}, \quad p,q \ \text{integer}, \tag{2}$$

that the topology of the phase space trajectories of the motion are strongly modified even in the limit of small perturbing amplitude E_0. The reason for this modification of the orbit topology is understood in terms of the linearity of the unperturbed oscillator. Since all of the nonlinearity occurs within the perturbation itself, the size of the local perturbation in action is independent of the perturbation strength. The limitation of this phenomenon with increasing nonlinearity of the original oscillator has been studied in the context of introducing nonlinearity by allowing a component of the wave propagation in the magnetic field direction.[4] A similar effect can be found by employing relativistically correct dynamics. A review of the problem can be found in ref. 5.

A motivation for the study of this problem is that of charged-particle heating by waves. For strong perturbations the higher order nonlinear interactions generate stochastic layers around the first order separatrices through which particles can diffuse in action, and therefore heat. Because this diffusion rate is related to the local strength of the perturbation, the original calculations, governed by interaction with a single wave as in (1), considered large values of E_0 and explored regions of the phase space (in energy) for which the resonant interaction was maximized.[2,3,5]

Recently a new look at this problem has been undertaken,[6] in which the single wave has been replaced by a wave packet

$$E(x,t) = E_0 \sum_{n=-\infty}^{\infty} \sin(kx - n\omega t). \tag{3}$$

This is equivalently represented by a periodic δ-function, kicking the particle, with period $T = 2\pi/\omega$. The differential equation for the motion then has a mapping representation[6]

$$\begin{aligned} u_{n+1} &= (u_n + K_\alpha \sin v_n)\cos\alpha + v_n \sin\alpha \\ v_{n+1} &= -(u_n + K_a \sin v_n)\sin\alpha + v_n \cos\alpha \end{aligned} \tag{4}$$

where $\alpha = \omega_c T$ is the rotation angle between kicks, $K_\alpha = (e/m)E_0 kT^2/\alpha$ is the stochasticity coefficient, and u and v are the normalized velocity components, $u = kv_x/\omega_c$, $v = kv_y/\omega_c$. The mapping is composed of a product of two involutions, a step change in u, followed by a rotation, and is therefore measure preserving. At a resonance we have $\alpha = 2\pi p/q$. Taking $p = 1$, for simplicity, we see that q is the number of δ-function kicks per gyroperiod.

In a series of papers, Zaslavski and associates have examined various aspects of the mapping.[6,7,8] There is an approximate q-fold rotational symmetry which becomes exact in the limit of $K_\alpha \to 0$. Furthermore, for $q = 2$, 3, 4, and 6, there is also an exact translational symmetry in this limit. The combination of these two symmetries insures that the phase space is tiled by the separatrix joining the unstable periodic points of the mapping. For other values of q, the separatrices are much more complicated, but for small K_α tend to produce structures that have a skeleton approximated by a q-fold rotation of a set of parallel lines. With finite K_α, higher order resonances produce stochastic layers of finite thickness.

The purpose of our study is to calculate the rate of diffusion through stochastic separatrix layers at finite K_α. The interest in this calculation is not to determine particle heating rates, since nonlinearities such as a component of k along $\hat{z}B_0$[4] or relativistic effects[9] will reintroduce energy-limiting KAM curves for small values of K_α. Our interest, rather, is to determine the effect of the divided phase space and the phase correlations on the global diffusion rate. These higher order effects can be studied for doubly periodic mappings,[10] such as the standard mapping, but only local approximations can be found for mappings which are periodic in phase, but not in action.[11] For the aperiodic mappings the existence of KAM barriers to diffusion limits the numerical calculation of diffusion rates. In contrast, for diffusion through a stochastic web the global rate of diffusion depends both on the internal phase space structure of the web and on the web boundaries. The effect of the internal structure can then be inferred from the global diffusion rate.

To investigate this effect most easily it is important to have a web with a stochastic layer that is globally uniform when averaged over a cell. To obtain this uniformity to order K_α we must limit ourselves to q-values with translation symmetry. The simplest of these values is q = 4, for which the map (4) reduces to the form

$$\begin{aligned} u_{n+1} &= v_n \\ v_{n+1} &= -(u_n + K_\alpha \sin v_n) \ . \end{aligned} \tag{5}$$

The twist can then be removed, to order K_α, by iterating the map four times, keeping only the lowest order terms, to obtain

$$\begin{aligned} v_{n+4} &= v_n - 2K_\alpha \sin u_n \\ u_{n+4} &= u_n + 2K_\alpha \sin v_{n+4} \ . \end{aligned} \tag{6}$$

The map (6) is again a product of two involutions and therefore measure preserving; it will be the fundamental mapping considered in the following sections. Although (6) was derived from (5) a subtle difference has arisen which becomes very important for the calculation of the separatrix width in the next section. That is, the map (5) has one kick per step or 4 kicks per gyroperiod while the map (6) has 2 kicks per step or two kicks per gyroperiod, each kick being twice as large. The first order structure is the same in both cases, but not the thickness of the separatrix layer which depends exponentially on the ratio of δ-function period to the period going around a cell.

The map (6), being measure preserving, has a Hamiltonian form[5,6]

$$H_4 = -2K_\alpha(\cos v + \cos u) - 2K_\alpha \cos u \sum_{\substack{n=-\infty \\ n\neq 0}}^{\infty} \cos \frac{n\alpha t}{4} \tag{7}$$

where the summation is the Fourier representation of the periodic δ-function. Since the lowest order oscillation about the fixed point has the frequency $\Omega_4 = 2K_\alpha$, for small K_α this frequency is very slow compared to the wave frequency. This allows averaging over the rapidly varying terms to obtain the averaged Hamiltonian[5,6]

$$\overline{H}_y = -2K_\alpha(\cos v + \cos u) \tag{8}$$

The averaged Hamiltonian is clearly 2π periodic with a separatrix web of straight lines given by[6]

$$v = \pm(u+\pi) + 2\pi m \tag{9}$$

It is the structure within this web, when the rapidly varying terms cannot be completely ignored, that interests us. Clearly this is significant for K_α sufficiently large that the nonlinear resonances between the fundamental frequency and the wave frequency become important.

In Fig. 1 the separatrix web is shown for a rather large value of $K_\alpha = 0.6$, in order to be able to see the web thickness. One thousand initial values of u and v were chosen within the stochastic region at the center of the figure, and were followed for 10^3 mapping iterations. The edge of the stochastic region is bounded by KAM curves within each mesh. Both the distortion of the separatrix from the straight line 45° grid, and the web thickness are clearly seen for this value of K_α.

In section 2 we consider the structure of the separatrix web. We use a combination of analytical and numerical calculations to obtain the important quantities such as the rotation frequency of a phase point around a mesh of the web and the thickness of the separatrix layer. We then use these results, in section 3, to calculate the rates of global diffusion through the web, as a function of K_α, and to compare these rates to numerically determined values.

We emphasize here that, although the diffusion has in common with higher dimensional Arnol'd diffusion the topological existence of a continuously connected web, the diffusion mechanisms and the diffusion rates are fundamentally different. For Arnol'd diffusion, motion across a stochastic layer, which is exponentially thin in the ratio of two frequencies associated with two degrees of freedom, drives exponentially slow diffusion along a stochastic layer in a third degree of freedom. In contrast, the diffusion rate studied here has a power law dependence on the corresponding frequency ratio, despite the exponentially thin layer width. This distinction was obscured in previous work in which the main interest was in the topology of the connected layer, rather than in the rate of diffusion through it.[6,9]

2. Structure of the stochastic layer

Near the separatrix of an oscillator which is perturbed by higher frequencies, the motion can be approximated by a separatrix mapping of the form[5]

$$\Delta w = w_0 \sin\theta \tag{10a}$$

$$\Delta\theta = 2\pi\tau(w)/m \tag{10b}$$

where w is the energy (or action) deviation from the separatrix, τ is the full period (in mapping steps) to traverse the web, and w_0 is an exponentially small function of the ratio Q_0 of the mapping period to the linearized mesh frequency, which can be expressed in terms of an Arnold-Melnikov integral in the form[5,12]

$$w_0 = c\, Q_0^2 \exp\left[-\frac{\pi Q_0}{2}\right], \tag{11}$$

with the constant of proportionality c to be determined. We do this numerically by relating w_0 to the border of stochasticity by use of the Chirikov criterion.[5,12] Expanding the mapping (10) about a periodic point

$$\tau(\overline{w}) = l \quad , \quad l \ integer \quad , \tag{12}$$

we obtain the standard mapping

$$\begin{aligned} \Delta I &= K_s \sin\theta \\ \Delta\theta &= I \end{aligned} \tag{13}$$

where

$$K_s = \frac{\pi}{K_\alpha}\frac{w_0}{\bar{w}} \ . \tag{14}$$

At the stochastic border the Chirikov criterion is $K_s = 1$, giving

$$\bar{w} \equiv w_1 = \pi w_0 / K_\alpha \ . \tag{15}$$

Substituting (11) in (15), with $Q_0 = \pi/K_\alpha$, we have

$$w_1 = \frac{\pi c}{K_\alpha^3} \exp\left[-\frac{\pi^2}{2K_\alpha}\right] \tag{16}$$

Since we shall only need to know the logarithmic value of w_1, a numerically determined value of c will be sufficient for our purposes.

In Fig. 2(a) we show a portion of the separatrix region near an unstable fixed point, which is blown up in Fig. 2(b). The last island chain before a mesh-bounding KAM curve corresponds, roughly, to the island chain satisfying $K_s = 1$. Because we must satisfy (12) exactly, at the fixed point, the criterion $K_s = 1$ cannot be satisfied exactly. However, since K_α varies significantly from island chain to island chain, a more general criterion for unequal island sizes will usually place the first KAM curve of the mesh at a w_1 greater than that given by (15). We discuss this further, below.

We can numerically determine the width of the stochastic region for the map (6) in two ways. Expanding (8) in u from an unstable fixed point, at (say) $u = \pi$, $v = 0$ we have

$$w \equiv \Delta H = K_\alpha u^2 \tag{17}$$

we then either put in a series of values of u, for a given K_α, and observe the transition from bounded to unbounded motion, or directly measure the distance (in u) to the edge of the stochastic layer. The two methods give quite similar results, shown for the first method, in Fig. 3, as the x's. In contrast, the separatrix thicknesses for the original mapping (4) are shown (plusses). These can be brought into correspondence with the reduced mapping (6) by reducing K_α (proportional to the mesh frequency) by a factor of 2 (circles), to keep the ratio of kicks to mesh frequency constant. A fit to (16) gives $c = 20$, which will be used in the following section.

We also need $\tau(w)$ for our diffusion calculation. Using (8), together with Hamilton's equations we can then obtain the period

$$\tau = \frac{2}{K_\alpha} \int_0^{\cos^{-1}(w_1-1)} \frac{du}{\sqrt{1-(w-\cos u)^2}} \tag{18}$$

where, as previously, w is the deviation in energy (or action) units from the value of H on the separatrix ($H_{sx} = 0$). The elliptic integral (18) is logarithmic near the separatrix, and has been found by numerical integration to be

$$\tau(w) \cong \frac{2}{K_\alpha}(2-\ln w) . \tag{19}$$

Referring again to Fig. 3, with $K_\alpha = 0.4$, the value of $w_1 \cong 4 \times 10^{-3}$, obtained from (16) corresponds, from (19) to $\tau(w_1) = 38$. That is, it takes 38 mapping iterations to traverse the mesh. Since the island chains occur in multiples of 4, we find the next main island chain closer to the separatrix corresponds to $\tau(w) = 42$. Inverting (19) we find $w_1 \approx 1.66 \times 10^{-3}$ with a corresponding $K_s \approx 2.4$, from (14). The result is that the next island chain closer to the separatrix, as seen in Fig. 2(b), exhibits a strong fourth harmonic resonance, and is well embedded within the stochastic sea. The process by which island chains become engulfed within the stochastic sea causes jumps in the value of w_1 at discrete values of K_α. However, the strong nonuniformity in neighboring island chains keeps the last KAM surface relatively constant with respect to the Chirikov criterion $K_s = 1$. The small variations may explain the wobble in the numerical values of $w_1(K_\alpha)$ in Fig. 3.

More important for our diffusion calculation, we see from Fig. 2b that the last KAM surface lies beyond the island chain whose center approximately satisfies the Chirikov criterion (15). This somewhat more than compensates for phase space area excluded from the stochastic region by the main island chain (and smaller islands). In the next section our diffusion calculation uses (15), which we shall see leads to a small systematic under-estimate of the asymptotic diffusion rate.

3. Diffusion rate and scaling

We now consider the central problem of the diffusion rate through a stochastic web. If the phase space density in the web is macroscopically uniform we expect a random process to govern the macroscopic diffusion over the cells. Assuming, that in each dimension, the probability of moving r displacements from the origin in N steps has the standard form[13]

$$P(r,N) = \left[\frac{2}{\pi N}\right]^{1/2} \exp\left[-\frac{r^2}{2N}\right] \tag{20}$$

then the rms distance traveled is $L_{rms} \equiv \langle L^2\rangle^{1/2} = L_{step}N^{1/2}$ where L_{step} is the fixed cell size. For our mesh we have $u_{step} = v_{step} = \sqrt{2}\,\pi$ with $N/2$ steps each in u and v, giving

$$L_{rms} = (\langle u^2\rangle + \langle v\rangle^2)^{1/2} = L_{step}N^{1/2} = \sqrt{2}\,\pi N^{1/2} \tag{21}$$

The diffusive nature of the spreading of initial conditions can be seen numerically from the relation between L_{rms} and the number of iterations of the mapping. This is plotted for two values of K_α in Fig. 4. After an initial transient during which time the initial conditions ergodically fill the stochastic region, the basic $L_{rms} \propto T^{1/2}$ dependence is evident, characteristic of a diffusive process.

The important physics is in the determination of the number of mapping periods that are required, on average, for a single random walk step. We make the following assumptions.

(1) The stochastic region is ergodic. This implies that the stochastically available canonical phase space out to the KAM barrier is uniformly occupied in the asymptotic (long time) limit.[14] This result has been shown numerically to be a good approximation in the regions of phase space where no islands exist.[15]

(2) As a first approximation we ignore the effect of islands on the calculation, assuming that the phase space is ergodic from the separatrix ($w = 0$) to the value $w = w_1$, satisfying the Chirikov criterion. As we have discussed, this a reasonable first order approximation, despite the existence of large islands near the border of stochasticity.

(3) In the small K_α limit, appropriate for the derivation of the fundamental map, the lowest order motion can be described by the continuous Hamiltonian (8), and the stochastic layer is sufficiently narrow that the period in the stochastic separatrix is everywhere governed by (19).

With these assumptions we calculate the rms spreading from

$$L_{rms} = \frac{L_{step} T^{1/2}}{(n\tau_{ave})^{1/2}} \tag{22}$$

where T is the number of iterations, τ_{ave} is the average rotation period, and n is the average number of rotations per separatrix crossing. The average period within the separatrix layer is

$$\tau_{ave} = \frac{1}{w_1} \int_0^{w_1} f(w)\tau(w)dw \tag{23}$$

where w_1 is the border of stochasticity (15). Since w is the canonical action, by assumption (1), $f(w) = 1$, and (23) can be integrated directly, using $\tau(w)$ from (19), to give

$$\tau_{ave} = \frac{2}{K_\alpha} (3 - \ln w_1) \tag{24}$$

The logarithmic singularity at $w = 0$ is sufficiently weak that $\tau_{ave} \approx \tau(w_1)$ as seen by comparing (24) to (19). Substituting (16) (with $c = 20$) in (24) we obtain

$$\tau_{ave} = \frac{\pi^2}{K_\alpha^2} + \frac{2}{K_\alpha} (3 - \ln 20\pi + 3\ln K_\alpha) . \tag{25}$$

For small values of K_α the first term dominates and $\tau_{ave} \propto 1/K_\alpha^2$. We compare the prediction of (25) with the numerically determined τ_{ave} in which 100 initial conditions were integrated over 8000 mapping periods, for each K_α, with the results, shown in Fig. 5, indicating excellent agreement.

To determine the number of rotations per separatrix crossing we put (15) in the form

$$\frac{w_1}{w_0} = \frac{\pi}{K_\alpha} \tag{26}$$

Because of the correlations near KAM boundaries it is not possible to calculate separatrix crossings directly from a random walk. However a simple phase space argument can be invoked to calculate the fraction of the phase space of the stochastic region that crosses the separatrix on each step of the separatrix map. The energy steps are given by $w_0 \sin\theta$, from (10a), such that the phase space within $w_0 \sin\theta$ of the separatrix, with $\sin\theta$ negative, crosses the separatrix on each mapping step. Phase randomization then insures that the phases are equally populated on each time step, such that the phase space crossing the separatrix on each step is $\int_{\pi}^{2\pi} w_0 \sin\theta = 2w_0$. Since the available phase space is $2\pi w_1$ a fraction $w_0/\pi w_1$ of the total phase space crosses on each separatrix mapping period. Since there are four such mapping periods per circulation period, using (26), an initial phase point takes a random walk step (separatrix crossing) in a number of circulation periods

$$n = \pi^2/4K_\alpha . \tag{27}$$

This result is compared with the numerically determined n in Fig. 6. In the numerical determinations 50 points were followed for 10^5 and 5×10^5 iterations for each K_α. The results indicate that for the longer numerical iteration, the number of iterations per jump is quite close to that predicted from (27), with the numerically determined slope somewhat less than the predicted K_α^{-1} dependence. These differences are qualitatively due to the correlations near the border of stochasticity and the deviations of the available phase space from the estimate in (26). The first effect is clearly seen to be of importance, numerically, since lower iteration numbers give shorter separatrix crossing times, resulting from the difficulty in penetrating into the phase space close to the KAM barrier. The penetration time into this highly correlated region is longer at small K_α, accounting for the decreased slope. For the second effect, since the actual w_1 lies above the value at $K_s = 1$, but the large island decreases the ergodicly available phase space, the deviations from the simple approximation (26) tend to cancel, resulting in relatively good agreement.

We substitute (25) and (27) in (22) to obtain the value of L_{rms} for any T. Defining the global diffusion rate as

$$D_{web} \equiv L_{rms}^2/T \tag{28a}$$

yields

$$D_{web} = \frac{8K_\alpha^3}{\pi^2+2K_\alpha(3-\ln 20\pi+3\ln K_\alpha)} \tag{28b}$$

Without any adjustable parameters L_{rms} from (28) (solid line) is compared to numerical calculations for 1000 initial conditions and for $T = 2^{16}$ iterations per initial condition (crosses), for each K_α, in Fig. 7. We also calculate L_{rms}, using the numerical separatrix crossing times from Fig. 6 (triangles). The difference between the crosses and triangles from the two numerical procedures is indicative of the breakdown of ergodicity on short time scales. That is, phase space trajectories from which the numerical diffusion rate is calculated employing 65,000 iterations, do not penetrate the phase space near the border of stochasticity as well as the trajectories from which the separatrix crossings are calculated, employing 5×10^5 iterations.

4. Conclusions and discussion

For a linear oscillator perturbed by a resonant periodic δ-function, some resonant ratios produce a stochastic web that globally has nearly uniform thickness in the small perturbation limit. This situation is convenient for studying global diffusion across a stochastic region with locally nonuniform diffusion. Invoking the theorem that the phase space of the resultant area preserving mapping should become uniformly filled, asymptotically, an analytic expression was derived for the global diffusion rate, in good agreement with the numerically observed diffusion. Remarkably, the long time correlations near the stochastic borders, characteristic of a divided phase space, do not impede the diffusion. Rather, the inability of trajectories, on shorter time scales, to fill the regions of phase space in which strong correlations exist, tends to increase the rate of intermediate-time-scale diffusion over the asymptotic value.

Although the linearity of the kicked oscillator leads to a connected grid in phase space, the diffusion rate is related to that in two-dimensional phase space, with the diffusion coefficient $D_{web} \equiv L_{rms}^2/T$ scaling as K_α^3, where K_α is a small perturbation parameter. In contrast, Arnol'd diffusion in a higher dimensional space has a diffusion rate along the main resonances which scales with the web thickness, and therefore as $D_A \propto \exp(-\text{const}/K_\alpha)$. Although not directly related to our present study, we point out that there is also an important topological difference between the Arnol'd web and the web studied here. In the Arnol'd web, generated by a small coupling perturbation, higher order resonances connect the stochastic web arbitrarily closely to all parts of the phase space, while leaving the total measure of the web exponentially small. In contrast, KAM surfaces disconnect almost the entire center of each mesh from the stochastic grid that surrounds them. The global rate of Arnol'd diffusion remains an open question.

The theoretical model that we have used gives a quite accurate estimate of the diffusion rate in the asymptotic limit because of two canceling effects in the estimation of the stochastic phase space available to the diffusing particles. Improvement in the analytic expressions are possible by introducing a correction in the ratio of w_1/w_0, in (15). This can be accomplished by adding the stochastic phase space beyond the last island and subtracting the excluded island phase space. The procedure is, however, K_α dependent in a complicated way.

It is clear that we have been discussing diffusion only within the stochastic web. For small K_α most of the phase space is bounded within the meshes by KAM curves and has no global diffusion. If a small additional extrinsically stochastic perturbation is added to the mapping, then the phase space in the mesh will diffuse at the extrinsic rate into the separatrix region of more rapid diffusion. Since the surrounding meshes have neither sources nor sinks, on an appropriately long time scale the local density within the meshes and in the bounding web will be the same. In this limit the overall diffusion rate is a product of the global separatrix rate and the ratio of phase space areas of intrinsic to extrinsic stochasticity; this latter ratio is proportional to w_1 in (15). For this combined extrinsic and intrinsic diffusion, treated in ref 6 in a different limit, the diffusion of the entire phase space is exponentially small in the ratio of driving frequency to mesh frequency.

Acknowledgements

This work was supported in part by the Office of Naval Research, contract N00014-84-K-0367.

References

[1] C. F. F. Karney, Phys. Fluids 21 1584 (1978); Phys. Fluids 22 2188 (1979).

[2] A. Fukuyama, H. Momota, R. Itatani, and T. Takizuka, Phys. Rev. Lett. 38 701 (1977).

[3] M. A. Malkov and G. M. Zaslavsky, Phys. Lett. 106A 257 (1984).

[4] A. J. Lichtenberg in *Intrinsic Stochasticity in Plasmas* G. Laval and D. Gresillon, Ed., Les Ed. de Physique, Courtaboeuf, Orsay (1979) p. 13.

[5] A. J. Lichtenberg and M. A. Lieberman, *Regular and Stochastic Motion*, Springer-Verlag, NY, (1983).

[6] G. M. Zaslavskii, M. Yu Zakharov, R. Z. Sagdeev, D. A. Usikov, and A. A. Chernikov, Soviet Physics, JETP 64 294 (1986).

[7] G. M. Zaslavskii, M. Yu Zakharov, R. Z. Sagdeev, D. A. Usikov, and A. A Chernikov, JETP Lett. 44 453 (1986).

[8] A. A. Chernikov, R Z. Sagdeev, D. A. Usikov, and G. M. Zaslavsky, Phys. Lett. 125 101 (1987).

[9] D. W. Longcope and R. N. Sudan, Phys. Rev. Lett. 59 1500 (1987).

[10] A. B. Rechester, M. N. Rosenbluth, and R. White, Phys. Rev. A23 2664 (1981).

[11] N. W. Murray, A. J. Lichtenberg, and M. A. Lieberman, Phys. Rev. A 32 2413 (1985).

[12] B. V. Chirikov, Phys. Reports 52 265 (1979).

[13] S. Chandrasekhar, Rev. Mod. Phys. 15 1 (1943).

[14] V. I. Arnol'd and A. Avez, *Ergodic Problems in Classical Mechanics* Benjamin, NY (1968).

[15] A. J. Lichtenberg and M. A. Lieberman, "Diffusion in Two Dimensional Mappings," Physica D, to be published.

Figure Captions

Fig. 1. A portion of the separatrix web for mapping (6) with $K_\alpha = 0.6$. One thousand initial conditions within the web were iterated 10^3 times to generate the web.

Fig. 2. Structure of the phase space in the neighborhood of an x-point of the stochastic web for $K_\alpha = 0.4$.

Fig. 3. Thickness of the stochastic layer, w_1 as a function of K_α, for the reduced mapping of Eq. 6 (crosses) and the original mapping of Eq. 4 (plusses).

Fig. 4. Illustrating the diffusive nature of the spreading of initial conditions, $L_{rms} \propto T^{1/2}$.

Fig. 5. Comparison of theoretical and numerical values of average mesh period.

Fig. 6. Comparison of theoretical and numerical values of number of revolutions per separatrix crossing.

Fig. 7. Comparison of theoretical and numerical values of $L_{rms} \propto D_{web}^{1/2}$ (for a fixed number of iterations).

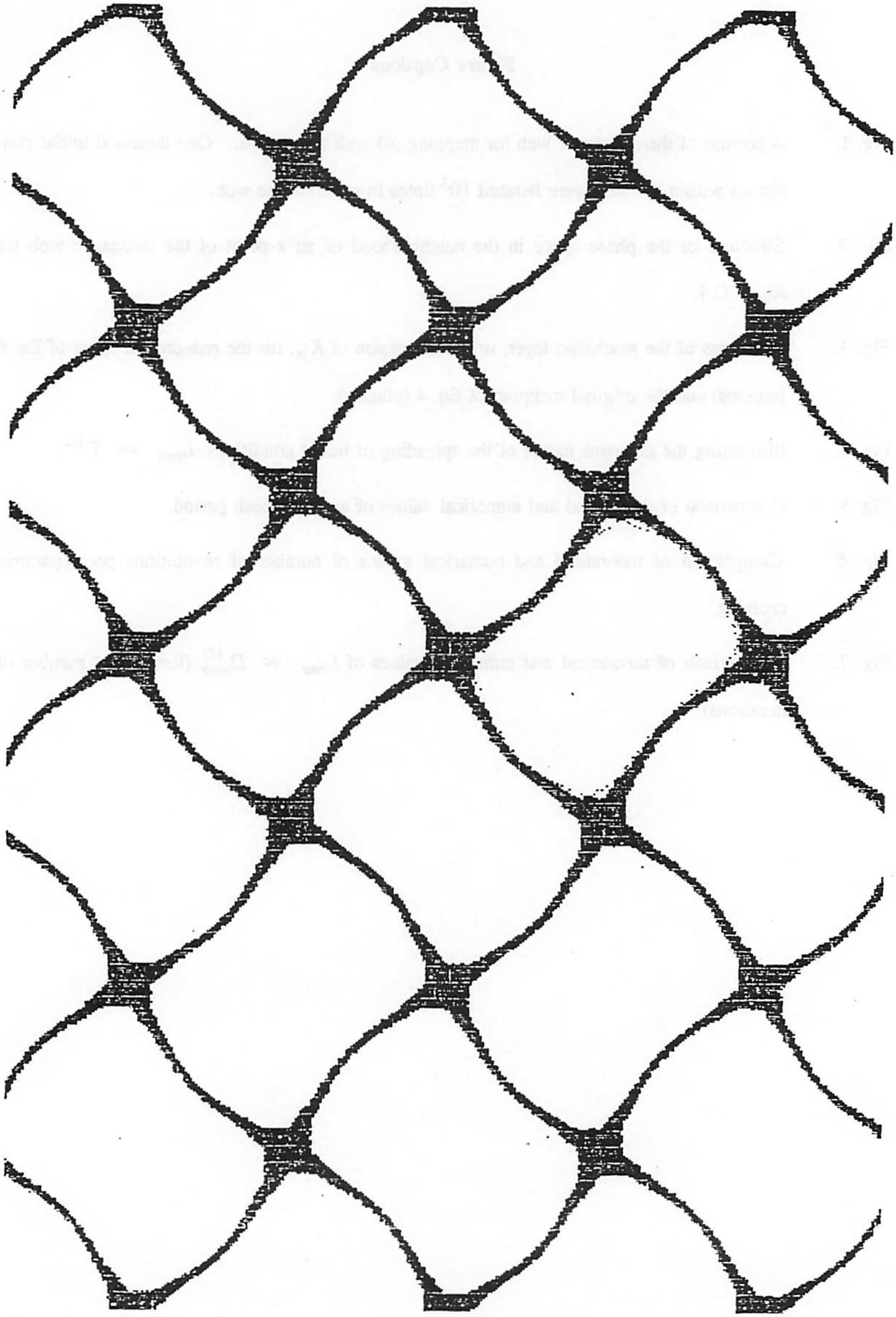

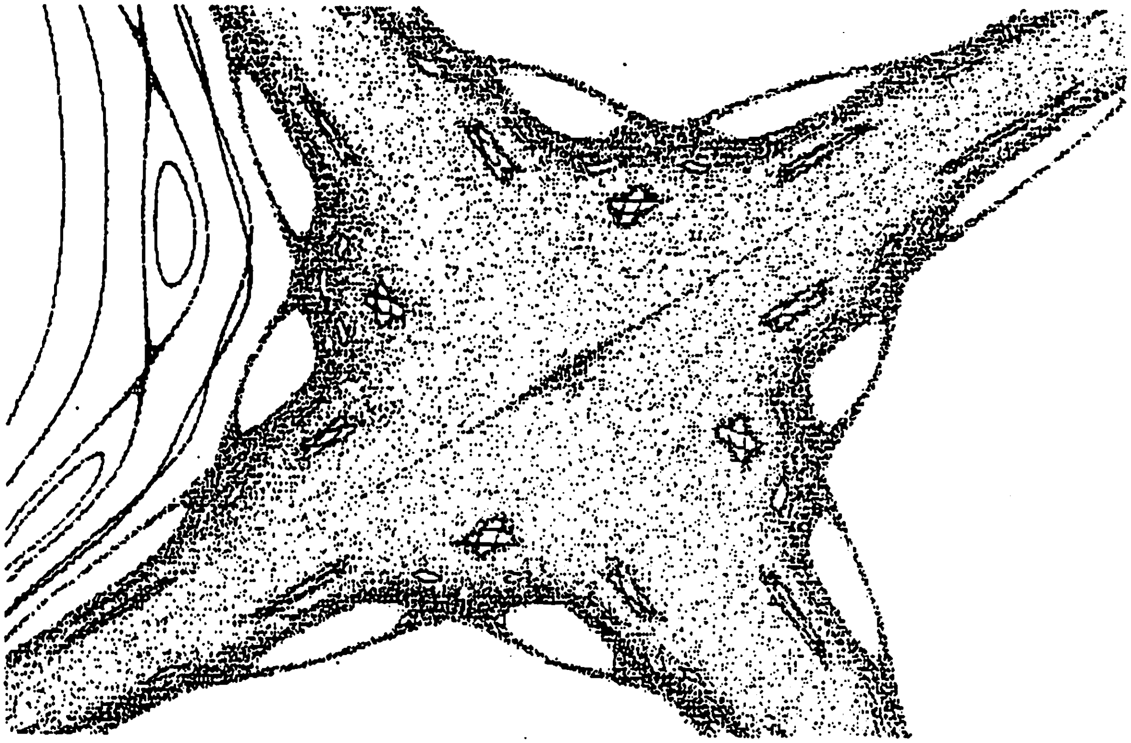

(a)

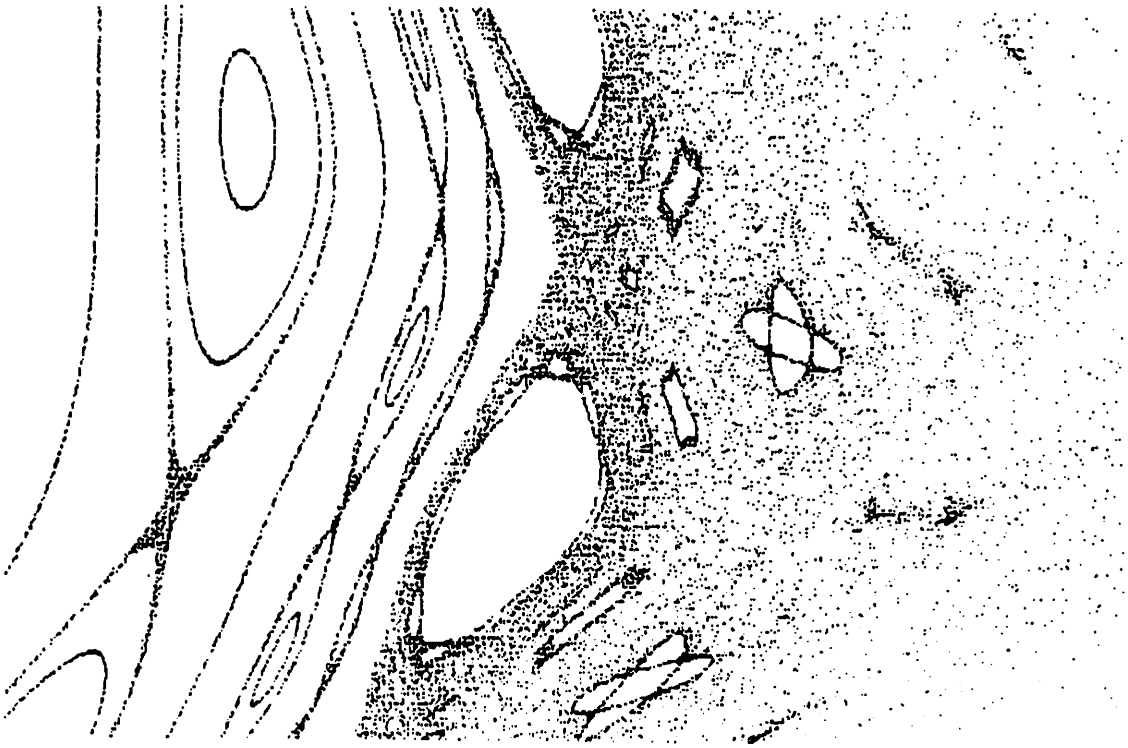

(b)

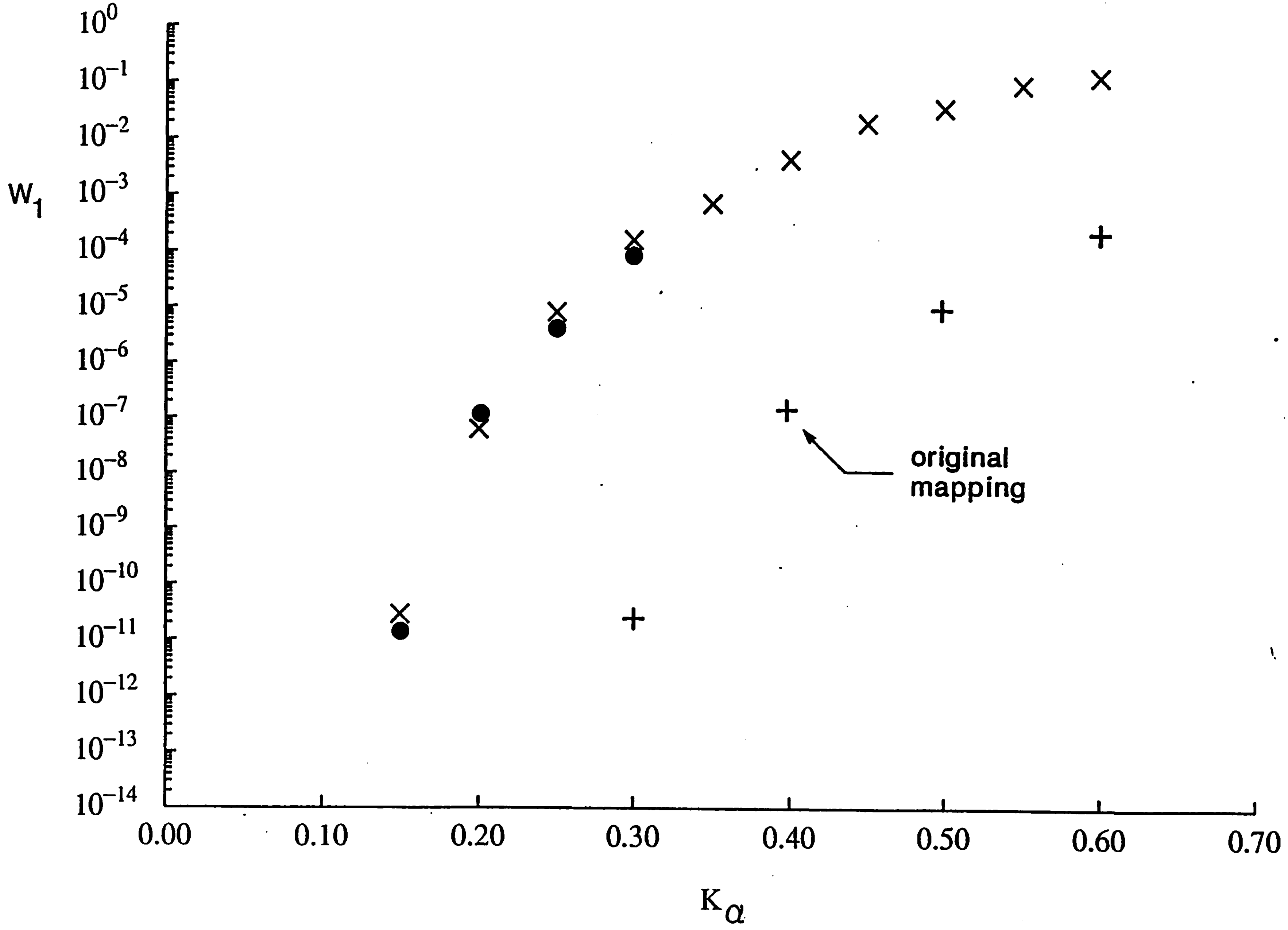

W_1
10^{0}
10^{-1}
10^{-2}
10^{-3}
10^{-4}
10^{-5}
10^{-6}
10^{-7}
10^{-8}
10^{-9}
10^{-10}
10^{-11}
10^{-12}
10^{-13}
10^{-14}
0.00
0.10
0.20
0.30
0.40
0.50
0.60
0.70
K_α
original mapping

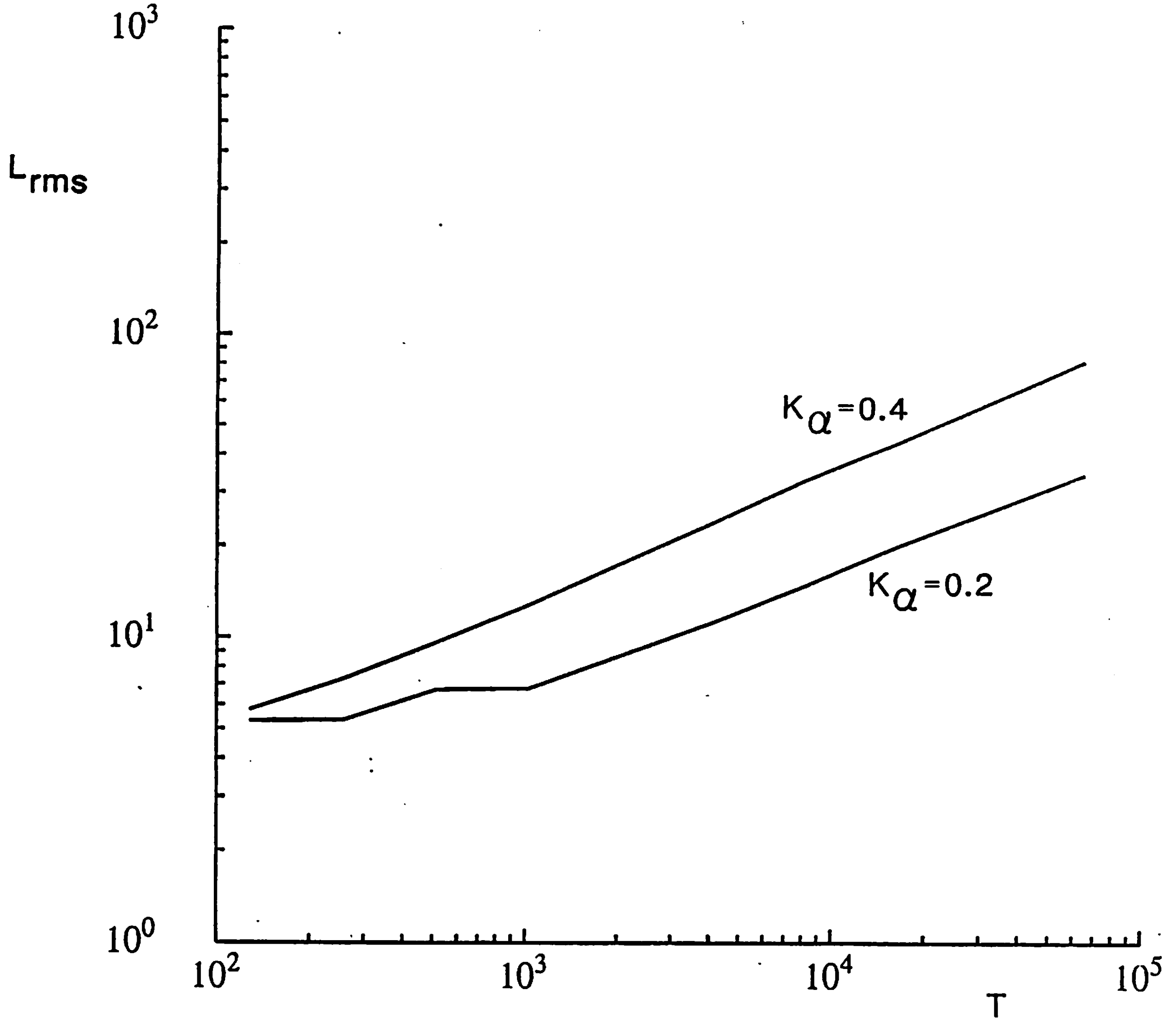
L_{rms}
10^3
10^2
10^1
10^0
10^2
10^3
10^4
10^5
T
$K_\alpha=0.4$
$K_\alpha=0.2$

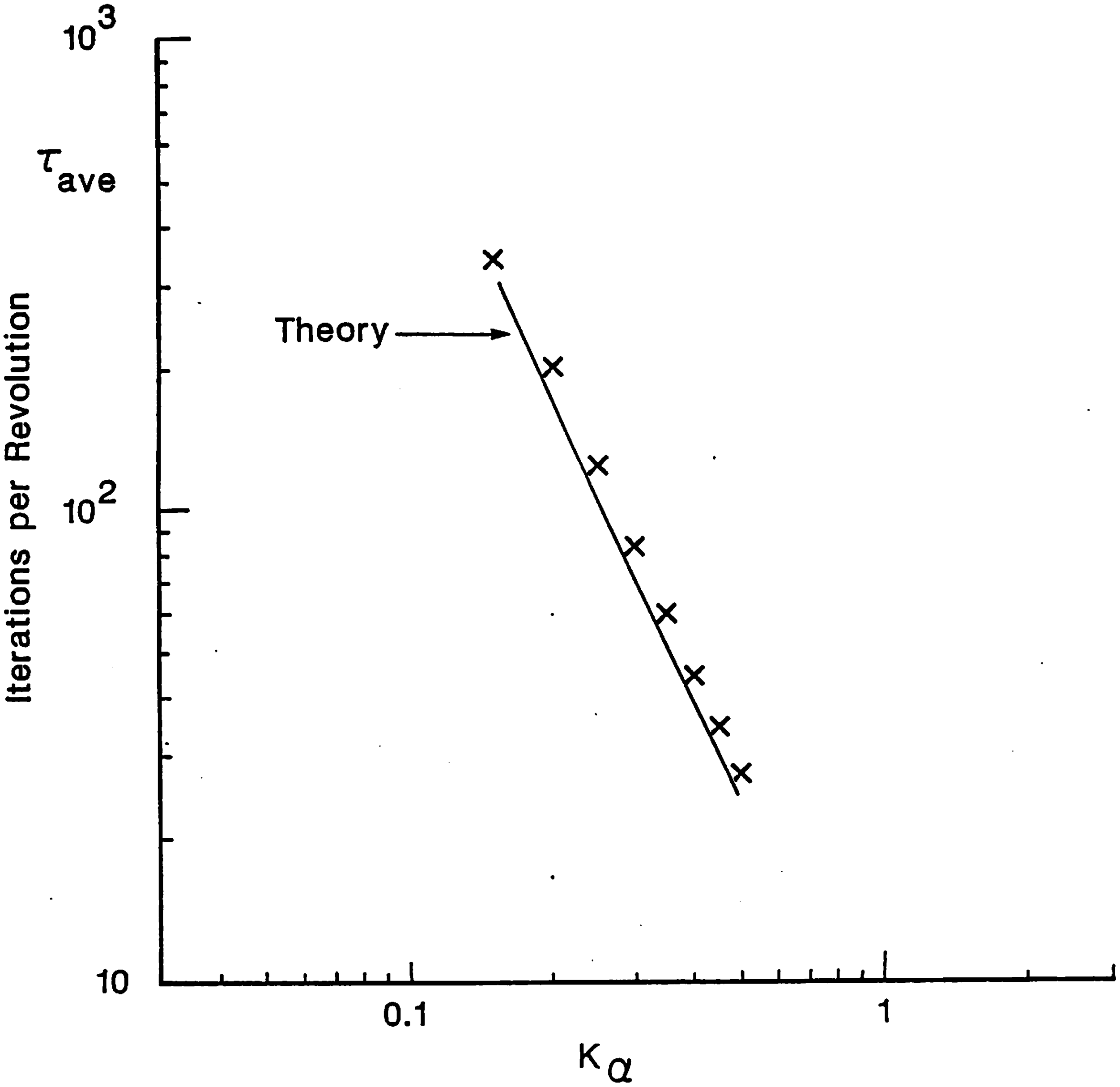
10^3
10^2
10
τ_ave
Iterations per Revolution
Theory
0.1
1
Kα

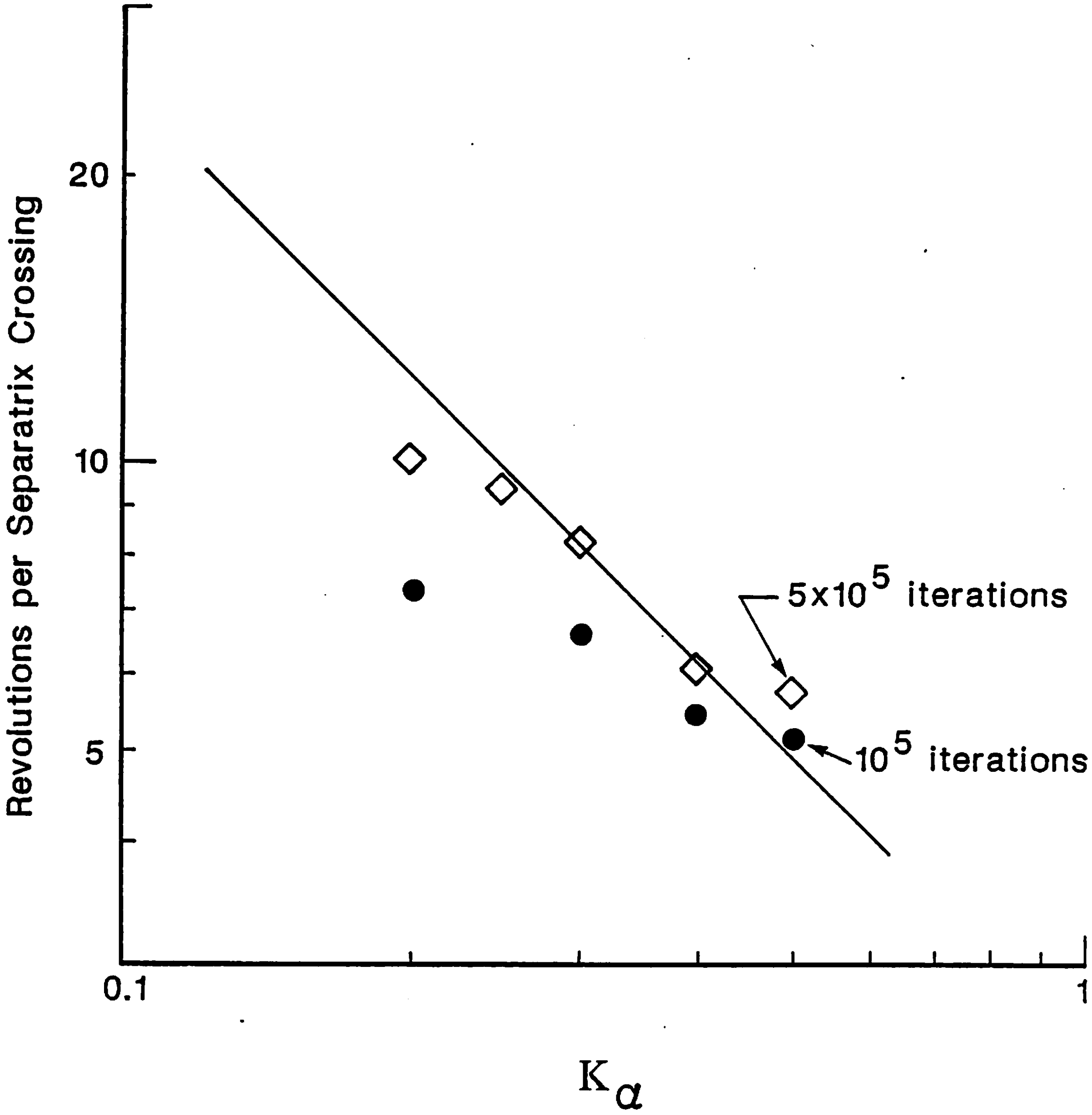
Revolutions per Separatrix Crossing
20
10
5
0.1
1
K_α
5×10^5 iterations
10^5 iterations

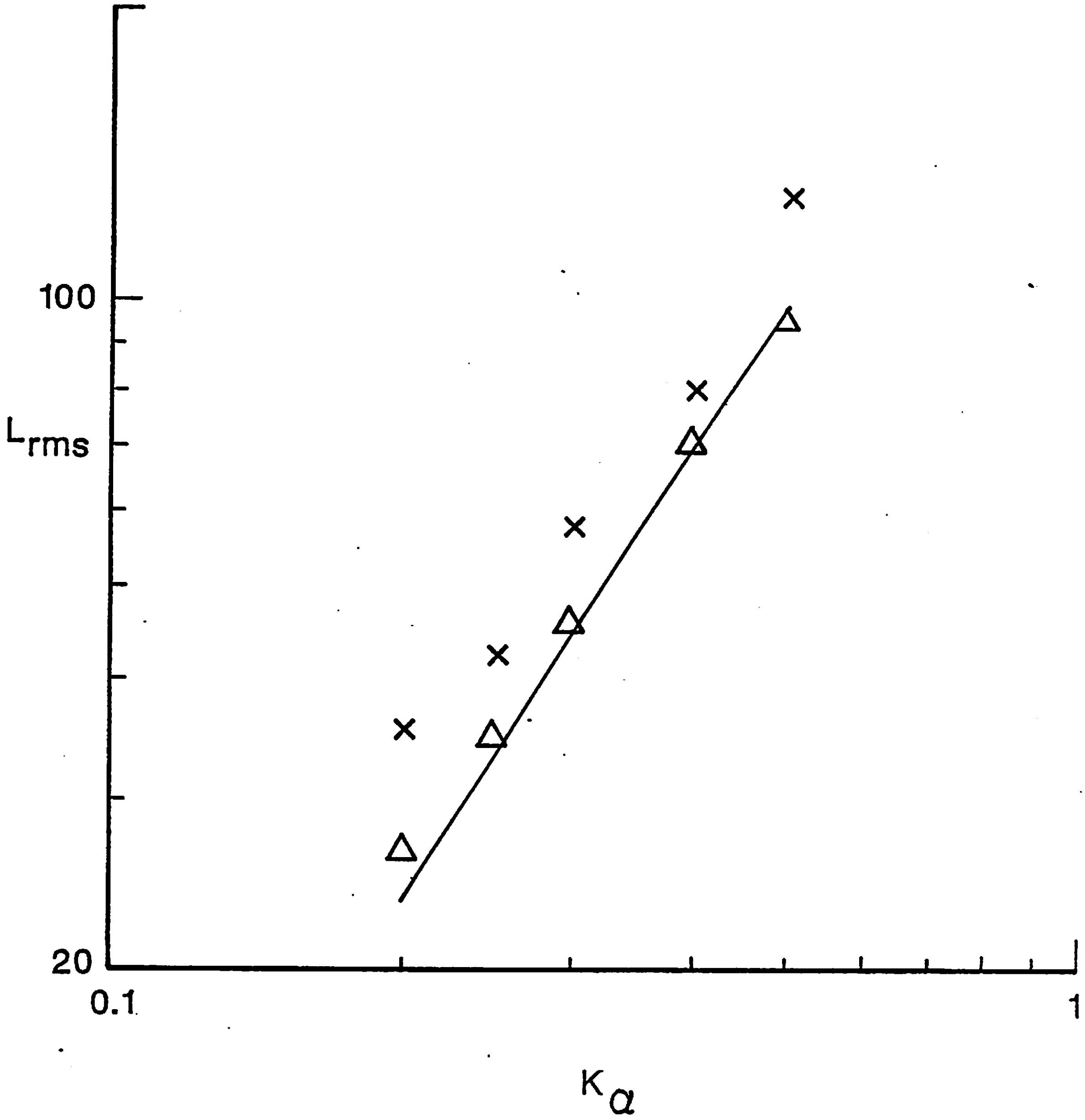
100
L_{rms}
20
0.1
1
K_{α}